Polycationic High-Spin States of One- and Two-Dimensional (Diarylamino)benzenes, Prototypical Model Units for Purely Organic Ferromagnetic Metals As Studied by Pulsed ESR/ Electron Spin Transient Nutation Spectroscopy

Kazunobu Sato,[†] Masafumi Yano,[†] Mutsuo Furuichi,[†] Daisuke Shiomi,[‡] Takeji Takui,*[,†] Kyo Abe,*[,†] Koichi Itoh,*[,‡] Akiji Higuchi,[§] Katsuhiko Katsuma,[§] and Yasuhiko Shirota*[,§]

Contribution from the Department of Chemistry and Department of Material Science, Faculty of Science, Osaka City University, Sumiyoshi-ku, Osaka 558, Japan, and Department of Applied Chemistry, Graduate School of Engineering/Faculty of Engineering, Osaka University, Suita, Osaka 565, Japan

Received September 26, 1996. Revised Manuscript Received May 15, 1997[⊗]

Abstract: Polycationic high-spin states of 1,3-bis(diarylamino)benzene and 1,3,5-tris(diarylamino)benzene as prototypical model units for organic ferromagnetic metals have been studied by cw and pulsed ESR spectroscopy. An electron spin transient nutation (ESTN) method as a novel technique based on pulsed ESR spectroscopy has been applied to the dicationic and tricationic high-spin states of them in glasses, unequivocally identifying the spin multiplicities of those molecules in the ground state to be triplet with the fine-structure parameters of $|D| = 0.007$ cm^{-1} and quartet with $|D| = 0.004$ cm^{-1}, $|E| = 0.0002$ cm^{-1}, and $g = 2.0023$, respectively, and concluding that the high-spin ground states originate from the topological pseudodegeneracy of the π-HOMOs which governs spin alignment in polycationic heteroatomic systems. It has been illustrated by the resolution enhancement inherent in the dimensional decomposition of 2D spectroscopy that magnetic-field-swept 2D ESTN spectroscopy is a powerful and facile method for spin identification and discrimination between different spin multiplicities in nonoriented systems. Also, ESTN phenomena have been treated in terms of both numerical calculation and perturbation theory. An analytical expression for the nutational motion has been derived.

Introduction

The last decade has found continuous interest in organic magnetics/molecule-based magnetism from both the pure and applied sciences. The conceptual proposals of organic magnetics in terms of noncharged molecular units with high-spin preference were made at early times,[1,2] and the first π-topological degeneracy giving rise to organic high-spin systems with $S = 2$ was shown 30 years ago.[3] The recent rapid development of this field based on high-spin chemistry is partly due to the rich variety of novel physical phenomena and properties which synthetic organomagnetic materials are expected to exhibit both macro- and mesoscopically[4] and partly due to their underlying potential applications as future technology in materials science such as spin-mediated molecular devices or electronics[4f,5,6] (defined as spinics or spintronics[5]).

Among diverse topics of organic magnetics, charged high-spin molecular systems generated by the hole or electron doping have recently drawn attention as models for studying the interplay between pluricharge fluctuation and spin polarization in homoatomic[7,8] and heteroatomic polycationic[9−15] high-spin molecular systems as well as in metal-bridge free stable

[†] Department of Chemistry, Osaka City University.
[‡] Department of Material Science, Osaka City University.
[§] Osaka University.
[⊗] Abstract published in *Advance ACS Abstracts,* July 1, 1997.

(1) (a) Morimoto, S.; Itoh, K.; Tanaka, F.; Mataga, N. *Prepr. Symp. Mol. Sci., Chem. Soc. Jpn.* **1968**, 76−77. (b) Mataga, N. *Theor. Chim. Acta* **1968**, *19*, 372−376. (c) Itoh, K. *Bussei* **1971**, *12*, 635−646. (d) Takui, T. Ph.D. Thesis, Osaka University, 1973. (e) Itoh, K. *Pure Appl. Chem.* **1978**, *50*, 1251−1259.

(2) (a) McConnell, H. M. *Proc. T. A. Welch Found. Chem. Res.* **1967**, *11*, 144. (b) McConnell, H. M. *J. Chem. Phys.* **1963**, *39*,1910−1911.

(3) (a) Itoh, K. *Chem. Phys. Lett.* **1967**, *1*, 235−238. (b) Wasserman, E; Murray, R. W.; Yager, W. A.; Trozzolo, A. M.; Smolinsky, G. *J. Am. Chem. Soc.* **1967**, *89*, 5076−5078.

(4) For a recent overview, see: (a) Miller, J. S., Dougherty, D. A., Eds. *Mol. Cryst. Liq. Cryst.* **1989**, *176*, 1−562. (b) *Advanced Organic Solid State Materials*; Chiang, L. Y., Chaikin, P. M., Cowan, D. O., Eds.; Materials Research Society: Pittburgh, PA, 1989; pp 3−92. (c) *Molecular Magnetic Materials*; Gatteschi, D., Kahn, O., Miller, J. S., Palacio, F., Eds.; Kluwer Academic Publishers: Dordrecht, The Netherlands, 1991; Vol. A198. (d) *Research Frontiers in Magnetochemistry*; O'Conner, C. J., Ed.; World Scientific: Singapore, 1993. (e) Iwamura, H., Miller, J. S., Eds. *Mol. Cryst. Liq. Cryst.* **1993**, *232/233*, 1−360/1−366. (f) Miller, J. S., Epstein, A. J., Eds. *Mol. Cryst. Liq. Cryst.* **1995**, *272/273*, 1−222/1−216. (g) *Ibid. 274/275*, 1−218/1−226. (h) *Molecular Magnetism: From Molecular Assemblies to the Devices*; Coronado, E.; Delhaès, P., Gatteschi, D., Miller, J. S., Eds.; Kluwer Academic Publishers: Dordrecht, The Netherlands, 1996; Vol. E321. (i) *Magnetism: A Supramolecular Function*; Kahn, O., Ed.; Kluwer Academic Publishers: Dordrecht, The Netherlands, 1996; Vol. C484. (j) *Molecule-Based Magnetic Materials: Theory, Technique, and Applications*; Turnbull, M. M., Sugimoto, T., Thompson, L. K., Eds.; American Chemical Society: Washington, DC, 1996; Vol. 644.

(5) (a) Takui, T.; Itoh, K. *Polyfile* **1990**, *27*, 49−59. (b) Takui, T.;Itoh, K. *J. Mater. Sci. Jpn.* **1991**, *28*, 315−335. (c) Takui, T. *Polyfile* **1992**, *29*, 48−49. (d) Takui, T. *Chemistry* **1992**, *47*, 167−174.

(6) (a) Miller, J. S.; Epstein, A. J. *Chemtech* **1991**, *21*, 168−169. (b) Landee, C. P.; Melville, D.; Miller, J. S. In *Molecular Magnetic Materials*; Gatteschi, D., Kahn, O., Miller, J. S., Palacio, F., Eds.; Kluwer Academic Publishers: Dordrecht, The Netherlands, 1991; Vol. A198.

(7) (a) Matsushita, M.; Momose, T.; Shida, T.; Teki, Y.; Takui, T.; Itoh, K. *J. Am. Chem. Soc.* **1990**, *112*, 4700−4702. (b) Matsushita, M.; Nakamura, T.; Momose, T.; Shida, T.; Teki, Y.; Takui, T.; Kinoshita, T.; Itoh, K. *J. Am. Chem. Soc.* **1992**, *114*, 7470−7475. (c) Matsushita, M.; Nakamura, T.; Momose, T.; Shida, T.; Teki, Y.; Takui, T.; Kinoshita, T.; Itoh, K. *Bull. Chem. Soc. Jpn.* **1993**, *66*, 1333−1342. (d) Nakamura, T.; Momose, T.; Shida, T.; Kinoshita, T.; Takui, T.; Teki, Y.; Itoh, K. *J. Am. Chem. Soc.* **1995**, *117*, 11292−11298. (e) Nakamura, T.; Momose, T.; Shida, T.; Kinoshita, T.; Takui, T.; Teki, Y.; Itoh, K. *Mol. Cryst. Liq. Cryst.* **1995**, *278*, 309−318.

(8) (a) Rajca, A.; Utamapanya, S.; Xu, J. *J. Am. Chem. Soc.* **1991**, *113*, 9235−9241. (b) Rajca, A. *Chem. Rev.* **1994**, *94*, 871−893 and references therein. (c) Rajca, A.; Rajca, S. *J. Am. Chem. Soc.* **1995**, *117*, 9172−9179.

S0002-7863(96)03372-0 CCC: $14.00

polyketone-based polyanionic molecular systems.[16] Also theoretically, the doping of organic high-spin systems has been studied referred to molecular design of purely organic magnetic metals and high-T_c organic superconductors, predicting the possible occurrence of the conversion from the low-spin states to the high spin-states (or vice versa) driven by spin polarization or double exchange mechanisms.[17−19]

One of the highlighted advances so far in organic magnetics and high-spin chemistry has been that the use of topological symmetry in the electron network of noncharged π-conjugated homoatomic hydrocarbons gives rise to the unlimited number of the degeneracy in π-nonbonding MOs (coined as topological degeneracy[1]) which contrasts with the limitation of usual orbital degeneracy in organic molecules as multinuclear centered systems. In this work, polycationic high-spin molecular systems under study have been considered as prototypical examples based on π-topology-mediated molecular design for one- and two-dimensionally extended super high-spin systems with multicharge. The systems studied, *meta*-linked or starburst molecules with triphenylamine branches, are of heteroatomic π-conjugation and expected to undergo dynamic spin polarization which is π-topologically controlled, leading to high-spin ground states. In this context, the present work is a pluricharge version of the topologically controlled through-bond approach to organic magnetics. Instead of "topological degeneracy" used for π-nonbonding MOs,[1] "super pseudodegeneracy" of π-HOMOs is used, which are located close to a zero energy level in units of resonance integral β; "pseudo" and "super" degeneracy originate in heteroatomic perturbation and topological symmetry of the π-conjugation network, respectively. These triphenylamine hyperbranched systems are prototypical examples for the present purposes, and they also have attracted interest from both the pure and applied sciences,[9−13] particularly related to functionalities like photoactivity and electronic activity for use in electronic devices.[20]

We have studied polycationic states of the *meta*-linked and starburst molecules based on (diarylamino)benzene using cw and pulsed ESR spectroscopy, emphasizing the unequivocal magnetic characterization of their high-spin ground states. The polycationic high-spin states have been studied so far using cw ESR spectroscopy by several groups.[9a,10a,12a,13] Nevertheless, electronic spin structures in their ground and nearby excited states are not fully expounded. In order to examine spin structures of high-spin systems, we developed the ESTN spectroscopy[21,22] which is applicable to randomly oriented or amorphous systems.[23] In the present work we deal with the polycationic high-spin ground states of *N*,*N*,*N*′,*N*′-tetra-4-anisyl-2,4-dimethyl-1,5-phenylenediamine (**1**) and *N*,*N*,*N*′,*N*′,*N*″,*N*″-hexa-4-anisyl-1,3,5-triaminobenzene (**2**)[10a] as the most fundamental 1D and 2D systems, respectively. The model systems **1** and **2** have the topological pseudo-2-fold and -3-fold degeneracy of π-HOMOs, respectively. The methyl and methoxy groups were introduced for increasing the chemical stability of the polycationic high-spin states. Efforts to stabilize *meta*-linked triphenylamine-based dications such as $\mathbf{1}^{2(\bullet+)}$ have been made.[9,12] The model system $\mathbf{1}^{2(\bullet+)}$ is the first example for 1D high-spin polycations. The introduction of functional groups governs the stability of polycationic species at ambient and low temperatures in solution. The chemical modification vs stability relationships studied by cyclic voltammetry will be published elsewhere.

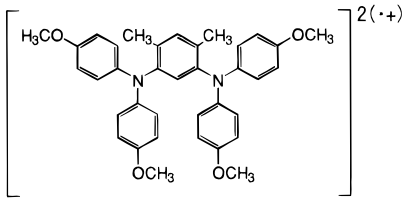

$\mathbf{1}^{2(\bullet+)}$

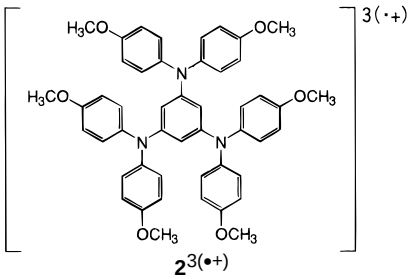

$\mathbf{2}^{3(\bullet+)}$

Pulsed FT-ESR/2D-ESTN (2D Electron Spin Transient Nutation) Spectroscopy for Nonoriented High-Spin Systems. ESTN spectroscopy is based on pulsed electron spin resonance to measure the spin Hamiltonian in terms of the rotating frame of microwave irradiation. In the ESTN measurements, the time evolution of the electron spin system in the presence of a microwave irradiation field $\mathbf{B}_1(t)$ and the static magnetic field $\mathbf{B}_0$ is observed in the rotating frame. We consider only the

(9) (a) Yoshizawa, K.; Chano, A.; Ito, A.; Tanaka, K.; Yamabe, T.; Fujita, H.; Yamauchi, J.; Shiro, M. *J. Am. Chem. Soc.* **1992**, *114*, 5994−5998. (b) Yoshizawa, K.; Tanaka, K.; Yamabe, T. *Chem. Lett.* **1990**, 1311−1314. (c) Yoshizawa, K.; Tanaka, K.; Yamabe, T. *Chem. Lett.* **1992**, 369−372. (d) Yoshizawa, K.; Tanaka, K.; Yamabe, T.; Yamauchi, J. *J. Chem. Phys.* **1992**, *96*, 5516−5522. (e) Yoshizawa, K.; Ito, A.; Tanaka, K.; Yamabe, T. *Solid State Commun.* **1993**, *87*, 935−937. (f) Ito, A.; Ohta, K.; Tanaka, K.; Yamabe, T.; Yoshizawa, K. *Macromolecules* **1995**, *28*, 5618−5625. (g) Ito, A.; Saito, T.; Tanaka, K. Yamabe, T. *Tetrahedron Lett.* **1995**, *36*, 8809−8812.

(10) (a) Stickley, K. R.; Blackstock, S. C. *J. Am. Chem. Soc.* **1994**, *116*, 11576−11577. (b) Stickley, K. R.; Blackstock, S. C. *Tetrahedron Lett.* **1995**, *36*, 1585−1588.

(11) Lee, J.; Chou, P. K.; Dowd, P.; Gralowski, J. J. *J. Am. Chem. Soc.* **1993**, *115*, 7902−7903.

(12) (a) Sasaki, S.; Iyoda, M. *Mol. Cryst. Liq. Cryst.* **1995**, *272*, 175−182. (b) Sasaki, S.; Iyoda, M. *Chem. Lett.* **1995**, 1011−1012.

(13) Wienk, M. M.; Janssen, R. A. J. *Chem. Commun.* **1996**, 267−268.

(14) Recently triplet states of *meta*-linked phosphoryl diradicals have emerged: Wienk, M. M.; Janssen, R. A. J.; Meijer, E. W. *Synth. Met.* **1995**, *71*, 1833−1834. Wienk, M. M.; Janssen, R. A. J. *J. Phys. Chem.* **1995**, *99*, 9331−9336.

(15) Recently, a high-spin ground-state anion from an intramolecularly spin-frustrated system has emerged: Nakamura, T.; Momose, T.; Shida, T.; Sato, K.; Nakazawa, S.; Kinoshita, T.; Takui, T.; Itoh, K.; Okuno, T.; Izuoka, A.; Sugawara, T. *J. Am. Chem. Soc.* **1996**, *118*, 8684−8687.

(16) A stable triketone-based intramolecularly spin-coupled trianion in the quartet ground state has been for the first time identified: Lazana, M. C. R. L. R.; Franco, M. L. T. M. B.; Shohoji, M. C. B. L. *J. Chem. Res. (S)* **1996**, 48.

(17) (a) Yamaguchi, K.; Toyoda, Y.; Fueno, T. *Chemistry* **1986**, *41*, 585−595. (b) Yamaguchi, K.; Toyoda, Y.; Fueno, T. *Synth. Met.* **1987**, *19*, 81−82. (c) Yamaguchi, K.; Takahara, Y.; Fueno, T.; Nakasuji, K.; Murata, I. *Jpn. J. Appl. Phys.* **1987**, *27*, L766−767. (d) Yamaguchi, K.; Namimoto, H.; Fueno, T.; Nogami, T.; Shirota, Y. *Chem. Phys. Lett.* **1990**, *166*, 408−412. (e) Yamaguchi, K. *Int. J. Quantum Chem.* **1990**, *37*, 167−175 and references therein.

(18) Yamanaka, S.; Kawakami, T.;Okumura, M.; Yamaguchi, K. *Chem. Phys. Lett.* **1995**, *233*, 257−265 and references therein.

(19) (a) Ikawa, A.; Mizouchi, H.; Fukutome, H. *Mol. Cryst. Liq. Cryst.* **1995**, *271*, 155−162 and references therein. (b) Mizouchi, H.; Ikawa, A.; Fukutome, H. *Synth. Met*; in press.

(20) (a) Shirota, Y.; Kobata, T.; Noma, N. *Chem. Lett.* **1989**, 1145−1148. (b) Ishikawa, W.; Inada, H.; Nakano, H.; Shirota, Y. *Chem. Lett.* **1991**, 1731−1734.

(21) Isoya, J.; Kanda, H.; Norris, J. R.; Tang, J.; Bowman, M. K. *Phys. Rev.* **1990**, *B41*, 3905−3913.

(22) Astashkin, A. V.; Schweiger, A. *Chem. Phys. Lett.* **1990**, *174*, 595−602.

(23) Sato, K.; Shiomi, D.; Takui, T.; Itoh, K.; Kaneko, T.; Tsuchida, E.; Nishide, H. *J. Spectrosc. Soc. Jpn.* **1994**, *43*, 280−291.

Scheme 1

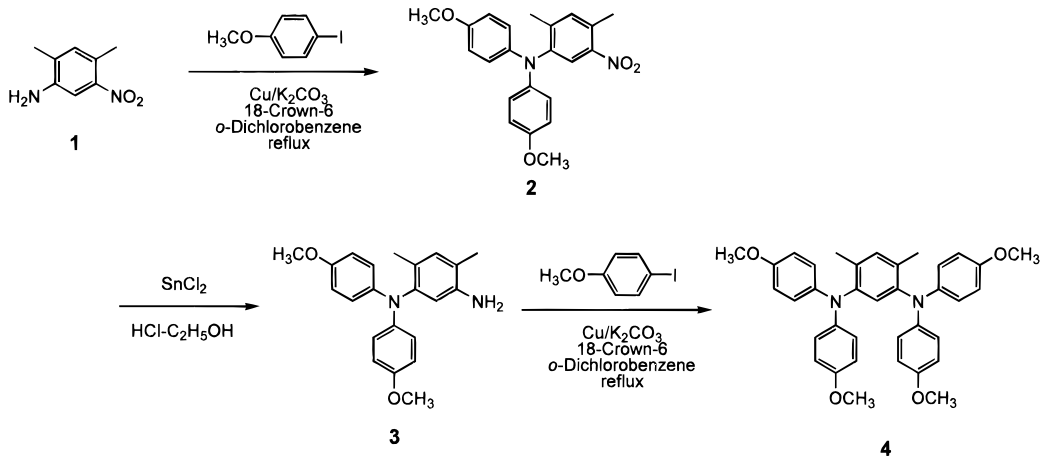

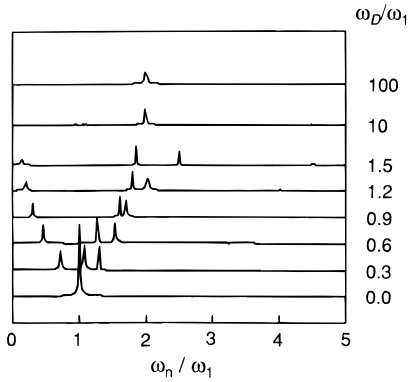

Figure 1. Dependence of the nutation spectra for an $|S = 3/2, M_S = 1/2\rangle \leftrightarrow |3/2, -1/2\rangle$ ESR transition on ω_D/ω_1. $\omega_E = 0$ was assumed.

electron Zeeman $\hat{H}_Z$ and fine-structure $\hat{H}_D$ terms in eq 5 for the ESTN analysis of high-spin systems. The rotating-frame Hamiltonian is given as

$$\hat{H}' = \Delta\omega S_z + [\omega_D(S_z^2 - \mathbf{S}^2/3) + \omega_E(S_x^2 - S_y^2)] - \omega_1 S_y \quad (1)$$

with $\Delta\omega = \omega_{M_W} - \omega_0$ and $\omega_1 = -\gamma_e B_1$, and where ω_D and ω_E stand for fine-structure parameters in units of frequency. The induction signal by the precessing magnetization of the spin system is given in proportion to

$$\langle S(t)\rangle = Tr\{\rho(t)S_+\} \quad (2)$$

which gives nutation frequencies for a given spin quantum number S by Fourier transformation. $\rho(t)$ is the density operator describing the state $|\psi'(t)\rangle$ of the system in the rotating frame. Nutation frequencies have been numerically computed in the present work below. The equilibrium density matrix was taken as an initial density matrix, $\rho(0)$.

We exemplify the nutation frequencies versus fine-structure parameter ω_D for high-spin systems with $S = 3/2$ as depicted in Figure 1. Figure 1 demonstrates the dependence of the nutation spectra for an $|S = 3/2, M_S = 1/2\rangle \leftrightarrow |3/2, -1/2\rangle$ ESR transition on ω_D/ω_1, where ω_1 stands for the strength B_1 of the microwave irradiation field ($\omega_1 = -\gamma_e B_1$). When ω_D is vanishing, the nutation spectrum has a single-frequency component with $\omega_n = \omega_1$. On the other hand, when $\omega_1 \ll \omega_D$, the spectrum gives $2\omega_1$ as the nutation frequency of the system. The coefficient c_n of $c_n\omega_1$ then depends on the spin quantum numbers S and M_S of the spin system as well as ω_D/ω_1.

The nutation frequency is also analytically evaluated in terms of the perturbation treatment of the rotating spin Hamiltonian. The signal given by eq 2 is proportional to

$$\langle S(t)\rangle = \sum_{M_S}\langle M_S - 1|\rho(0)|M_S\rangle[S(S+1) - M_S(M_S-1)]^{1/2}\exp[it\omega_D(2M_S - 1) + \omega_1 t[S(S+1) - M_S(M_S-1)]^{1/2}] \quad (3)$$

where only the ω_D term in $\hat{H}_D$ remains in the first-order approximation. Thus, in the extremely weak limit of the microwave irradiation field ($\hat{H}_1 \ll \hat{H}_D$), the nutation frequency is expressed as

$$\omega_n = [S(S+1) - M_S(M_S-1)]^{1/2}\,\omega_1 \quad (4)$$

for an $|S, M_S\rangle \leftrightarrow |S, M_S - 1\rangle$ ESR allowed transition.[21−23] The nutation frequency depends on S and M_S as well as ω_1. Note that this weak limit condition is satisfied under ordinary experimental conditions.

The ESTN method was first applied by Isoya *et al.*,[21] and Astashkin and Schweiger,[22] to single-crystal systems to interpret a distorted local site of Ni(II) ($S = 3/2$), and to identify fine-structure ESR transitions from paramagnetic transition metal ions, respectively. We have extended the ESTN technique to a wide variety of nonoriented systems, inorganic or organic including mixtures of high-spin oligomers/polymers.[23] ESTN measurements can be applied to any swept magnetic field in nonoriented systems, all the orientations of which contribute the corresponding nutation frequency. In this work we have developed magnetic-field-swept 2D ESTN spectroscopy which deserves to enhance spectral resolution in nonoriented systems. The field-swept 2D presentation is of essential importance in the ESTN spectroscopy in nonoriented systems, as described below. The ESTN spectroscopy is essentially free from spectral simulation for randomly oriented systems in order to identify S and M_S of high-spin systems.

Experimental Section

Materials. Melting points were determined on a micro-hot-stage and were uncorrected. IR spectra were taken on a JASCO A-102 IR spectrometer. ^{1}H (400 MHz) and ^{13}C NMR (100 MHz) spectra were recorded on JEOL 400 MHz and Hitachi 100 MHz instruments. *N,N,N′,N′*-Tetra-4-anisyl-2,4-dimethylphenylenediamine (**4**) was synthesized according to Scheme 1. *N,N,N′,N′,N″,N″*-hexa-4-anisyl-1,3,5-triaminobenzene was synthesized using the reported method.[10a,20b] Only new compounds are described below.

Chart 1. Three-Pulse Sequence Applied for ESTN Measurements.

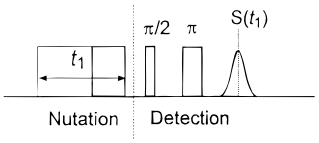

***N,N*-Di-4-anisyl-5-nitro-2,4-xylidine (2).** A mixture of 1 g (0.006 mol) of 5-nitro-2,4-xylidine,[24] 4.23 g (0.018 mol) of *p*-iodoanisole, copper powder (1.4 g), potassium carbonate (6.8 g), and 18-crown-6 ether (0.5 g) in *o*-dichlorobenzene (100 mL) was heated under reflux in argon atmosphere for 12 h. The mixture was filtered off, washed with water (100 mL × 2), and dried over sodium sulfate. The solvent was distilled off under reduced pressure. The obtained crude orange oil was used without further purification for the following reaction. ^{1}H NMR ($CDCl_3$): δ 3.81 (s, 6H), 6.84 (d, 4H, J = 8.56 Hz), 7.08 (d, 4H, J = 8.56 Hz), 7.13−7.66 (m, 4H). IR (Nujol): 1620, 1520 cm^{-1}.

***N,N*-Di-4-anisyl-2,4-dimethylphenylenediamine (3).** A mixture of *N,N*-di-4-anisyl-5-nitro-2,4-xylidine, 2.3 g (0.01 mol) of tin dichloride, and 5 mL of hydrochloric acid in ethanol (100 mL) was heated under reflux for 2 h. The mixture was poured onto ice-water containing potassium carbonate and extracted with chloroform (100 mL × 2). The organic phase was washed with water (100 mL × 2) and dried over sodium sulfate. The solvent was distilled off under reduced pressure. The obtained crude yellow oil was used without further purification for the following reaction. ^{1}H NMR ($CDCl_3$): δ 3.77 (s, 6H), 6.18−6.34 (m, 3H), 6.80 (d, 4H, J = 8.56 Hz), 6.93 (t, 1H, J = 7.92 Hz), 7.02 (d, 4H, J = 8.56 Hz). IR (Nujol): 3500, 3420 cm^{-1}.

***N,N,N′,N′*-Tetra-4-anisyl-2,4-dimethylphenylenediamine (4).** A mixture of *N,N*-di-4-anisyl-2,4-dimethylphenylenediamine, 4.23 g (0.018 mol) of *p*-iodoanisole, copper powder (1.4 g), potassium carbonate (6.8 g), and 18-crown-6 ether (0.5 g) in *o*-dichlorobenzene (100 mL) was heated under reflux in argon atmosphere for 12 h. The mixture was filtered off, washed with water (100 mL × 2), and dried over sodium sulfate. The solvent was distilled off under reduced pressure. The crude mixture was purified by chromatography on silica gel using chloroform, giving 0.44 g of white powder (total yield 13%). Mp: 121−122 °C. ^{1}H NMR ($CDCl_3$): δ 1.97 (s, 6H), 3.75 (s, 12H), 6.71 (d, 8H, J = 9.16 Hz), 6.82−6.84 (m, 9H), 7.02 (s, 1H). ^{13}C NMR ($CDCl_3$): δ 18.2, 55.5, 114.4, 122.6, 129.2, 132.8, 132.9, 134.5, 141.6, 154.2. IR (Nujol): 1510 cm^{-1}. MS: *m/e* 560. Anal. Calcd for $C_{36}H_{36}N_2O_4$: C, 77.12; H, 6.47; N, 5.00. Found: C, 76.75; H, 6.44; N, 4.89.

Generations of the Polycationic States of 1 and 2. Hole doping of neutral diamagnetic molecules can be carried out in an either wet or dry process. The latter involves γ-radiolyses in solids,[7] but it does not allow plurihole doping per molecule under usual conditions. For the plurihole doping, we adopted a wet process, described below, chemical oxidation in solution, which allows multiple-step hole doping and makes cationic molecules undergo the stabilization/relaxation of their molecular structure upon the hole doping in the presence of counteranions.

The polycationic high-spin molecules $\mathbf{1}^{2(\bullet+)}$ and $\mathbf{2}^{3(\bullet+)}$ were generated by chemical oxidation of the parent molecules **1** and **2** in dichloromethane containing tetra-*n*-buthylammonium tetrafluoroborate, *n*-Bu_4NBF_4, and lead tetraacetate. A small amount of trifluoroacetic anhydride was also dropped into the dichloromethane solution for performing the complete oxidation process in generating the polycations as described in the previous literature.[9a] The use of trifluoroacetic anhydride stabilizes the polycationic high-spin states of the (diarylamino)benzenes.

ESR/ESTN (Electron Spin Transient Nutation) Measurements. X-band cw ESR measurements were carried out on both JEOL JES-FE2XG and Bruker ESP300 spectrometers, equipped with JEOL ES-DVT2 and Oxford ESR910 temperature controllers, respectively. Pulsed ESR measurements were carried out on a Bruker ESP380 FT-ESR spectrometer with a dielectric resonator and a 1 kW traveling wave tube amplifier for microwave excitation.

(24) Keiderer, E. C.; Adams, R. *J. Am. Chem. Soc.* **1931**, *53*, 1575−1580.

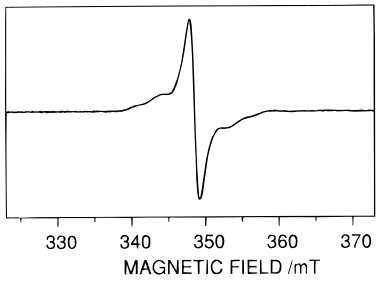

Figure 2. Powder-pattern ESR spectrum of the polycationic state of **1** observed at 7 K. The microwave frequency was 9.77375 GHz.

The ESTN experiments were performed by the three-pulse sequence shown in Chart 1, which consists of a nutation pulse (for microwave excitation) and a pair of $\pi/2-\pi$ pulses (for detection). We adopted a four-step phase cycling, monitoring the peak of a two-pulse Hahn echo, $S(t_1)$, after the nutation pulse with a different pulse length t_1. Two-dimensional (2D) ESTN spectra were constructed as a function of the swept magnetic field.

Computer Simulations of Solution and Powder-Pattern ESR Spectra. The spin Hamiltonian is generally given by

$$\hat{H} = \hat{H}_{eZ} + \hat{H}_D + \hat{H}_{nZ} + \hat{H}_{hf} + \hat{H}_Q$$
$$= \hbar^{-1}\beta\tilde{\mathbf{B}}_0\cdot\mathbf{g}\cdot\mathbf{S} + \hbar^{-1}\tilde{\mathbf{S}}\cdot\mathbf{D}\cdot\mathbf{S} + \hbar^{-1}\beta_n\tilde{\mathbf{B}}_0\cdot\mathbf{g}_n\cdot\mathbf{I} + \hbar^{-1}\tilde{\mathbf{S}}\cdot\mathbf{A}\cdot\mathbf{I} + \hbar^{-1}\tilde{\mathbf{I}}\cdot\mathbf{Q}\cdot\mathbf{I} \quad (5)$$

where $\hat{H}_{eZ}$, $\hat{H}_D$, $\hat{H}_{nZ}$, $\hat{H}_{hf}$, and $\hat{H}_Q$ have the usual meaning. In a solution ESR spectrum, anisotropic interactions vanish and the effective Hamiltonian is described by

$$\hat{H} = \hbar^{-1}g\beta\tilde{\mathbf{B}}_0\cdot\mathbf{S} + \hbar^{-1}g_n\beta_n\tilde{\mathbf{B}}_0\cdot\mathbf{I} + \hbar^{-1}a\tilde{\mathbf{S}}\cdot\mathbf{I} \quad (6)$$

The spectral simulations of solution and powder-pattern ESR spectra were performed using a homemade software[25] as well as a simulation software, WIN-EPR *Sim Fonia* by Bruker Instruments, Inc. The former is based on the eigenfield method and direct numerical diagonalization of the spin Hamiltonian. The latter is based on the second-order perturbation treatment using eqs 6 and 5 for the solution and powder-pattern simulations, respectively.

Results and Discussion

Polycationic State of *N,N,N′,N′*-Tetra-4-anisyl-2,4-dimethyl-1,5-phenylenediamine (1). The powder-pattern cw ESR spectrum of the polycationic state of **1** observed at 7 K is shown in Figure 2. There appeared five broad overlapping lines in an allowed ESR transition region. The central intense line suggested the occurrence of $\mathbf{1}^{1(\bullet+)}$ as a doublet species, the overall spectrum not allowing one to characterize the polycationic spin state unequivocally. In order to enhance a spectroscopic resolution with emphasizing S/M_S-discrimination, we have measured the ESTN phenomena using the pulsed ESR technique.

Figure 3 shows a contour plot of the 2D ESTN spectra observed at 5 K. The intense nutation frequency peak observed at 348 mT and two peaks at 345 and 351 mT in the wing are at 15.3 and 23.1 MHz, respectively. The nutation frequency expected for $|1, 0\rangle \leftrightarrow |1, \pm1\rangle$ transitions of a triplet state is $\sqrt{2}\omega_1$ from eq 4. At the central $g \approx 2$ field in which both ESR transitions are excited at the same time, the frequency is expected to be ω_1 because of a complete excitation. A frequency ratio of 23.1/15.3 corresponds to that of $\sqrt{2}/1$ expected for a triplet state from eq 4. It should be noted that

(25) Takui, T.; Sato, K.; Shiomi, D.; Itoh, K. In *Molecule-Based Magnetic Materials: Theory, Technique, and Applications*; Turnbull, M. M., Sugimoto, T., Thompson, L. K., Eds.; American Chemical Society: Washington, DC, 1996; Vol. 644, Chapter 6.

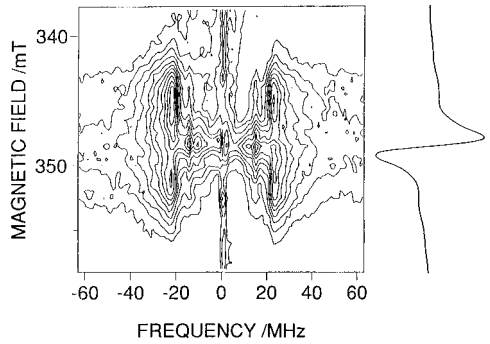

Figure 3. Contour plot of the field-swept 2D ESTN spectra of $\mathbf{1}^{2(\bullet+)}$ and the conventional field-swept ESR spectrum (on the right) observed at 5 K. ω_1 corresponds to about 15.3 MHz.

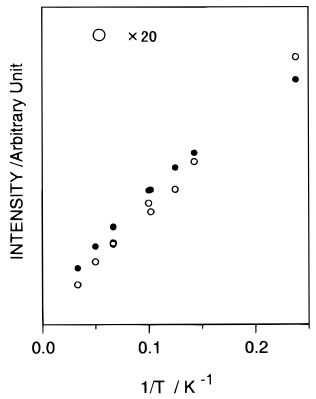

Figure 4. Temperature dependence of the signal intensities of $\mathbf{1}^{2(\bullet+)}$. Filled and open circles denote the signal intensities at 345.0 and 341.0 mT, respectively.

ω_n attributable to a spin doublet is ω_1 because of vanishing ω_D. The intensity of the peak observed at 348 mT was much stronger than that expected for the triplet state, indicating that signals due to doublet impurities were overlapping at 348 mT. The powder-pattern ESR spectrum, therefore, consisted of the triplet and doublet species that were attributed to the dication of **1** and the doublet impurities including the monocation of **1**, respectively.

The temperature dependence of the signal intensities was examined in order to determine whether the triplet state of $\mathbf{1}^{2(\bullet+)}$ was a ground or thermally excited state. As in the observed ESR spectra as shown in Figure 2 the triplet signal overlapped with doublet ones, we compared the relative intensities of the signals observed at 345.0 mT (central peak) and 341.0 mT in the wing. The temperature dependence of the signal intensities is shown in Figure 4. The temperature dependence of the triplet signal depends linearly on that of the central peak that dominantly consisted of doublet impurities. It is therefore concluded that the dicationic state of **1** is a ground-state triplet.

For the triplet state of $\mathbf{1}^{2(\bullet+)}$, the fine-structure parameter $|D|$ was determined to be 0.007 cm^{-1} from a splitting between the Z transitions in the ESR spectrum. Determination of the E value was erroneous because of low spectral resolution. The $|D|$ value is close to those (0.0064−0.0079 cm^{-1}) of neutral high-spin molecules with the similar electronic spin structure which have been reported so far,[8,26−28] suggesting that the $\pi-\pi$ two-center spin−spin interactions and dynamic spin polarization dominate spin alignment, and in terms of $|D|$ values charge fluctuation does not apparently affect the spin polarization mechanism.

The magnitude of the D value of $\mathbf{1}^{2(\bullet+)}$ is consistent with that of $\mathbf{2}^{3(\bullet+)}$ if the projection factor $2S-1$ for D values is considered. The value of $(2S-1)|D| = 0.008$ ($S = 3/2$, $|D| = 0.004$ cm^{-1} for $\mathbf{2}^{3(\bullet+)}$: see below) can be compared with $(2S-1)|D| = 0.007$ ($S = 1$) for $\mathbf{1}^{2(\bullet+)}$, neglecting differences in molecular structure. This comparison is based on order-of-magnitude estimation, nevertheless indicating that the similar values of $(2S-1)|D|$ are due to the similarity of the spin structure between $\mathbf{1}^{2(\bullet+)}$ and $\mathbf{2}^{3(\bullet+)}$. In this context, detection and identification of $\mathbf{2}^{2(\bullet+)}$ are interesting to understand the molecular structures vs charge fluctuations of these cationic states with counteranions.

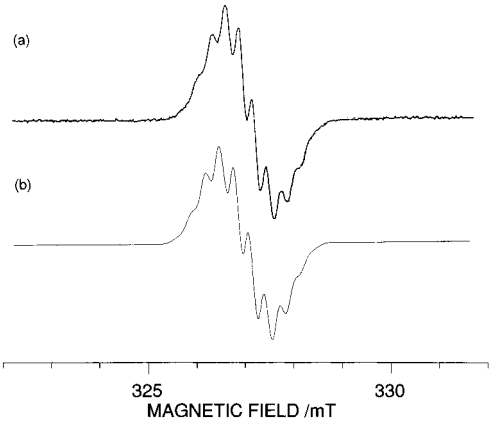

Figure 5. (a) Solution ESR spectrum of the cationic state of **2** observed at 203 K in a dichloromethane solution. (b) Simulated ESR spectrum with $\Delta B_{1/2} = 0.285$ mT, $a_N = 0.3$ mT (for three nitrogen atoms), and $a_H = 0.26$ mT (for three hydrogen atoms of the central phenyl ring). The hyperfine coupling parameters for the three equivalent nitrogen and hydrogen atoms were taken into account.

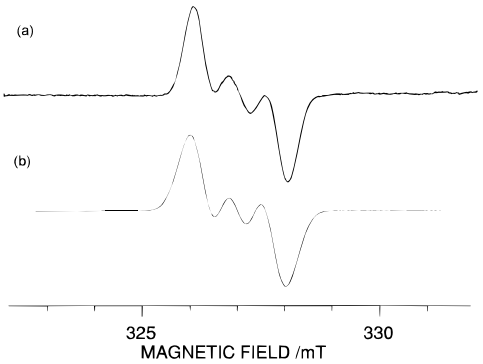

Figure 6. (a) Solution ESR spectrum of the cationic state of **2** observed at ambient temperature in a dichloromethane solution. (b) Simulated ESR spectrum with $\Delta B_{1/2} = 0.64$ mT, $a_N = 0.7$ mT (for one of three nitrogen atoms), and $a_N = 0.01$ mT (for other nitrogen atoms). The hyperfine coupling parameters for the three nitrogen atoms were taken into account.

Solution ESR Spectra of the Cationic States of *N,N,N′,N′,N″,N″*-Hexa-4-anisyl-1,3,5-triaminobenzene (2). Figures 5 and 6 show ESR spectra of the cationic state of **2** observed in a dichloromethane solution. The solution ESR spectrum in Figure 5 was observed at 203 K after the chemical oxidation process by tetra-*n*-buthylammonium tetrafluoroborate, *n*-Bu_4NBF_4, and lead tetraacetate with a small amount of trifluoroacetic anhydride, and that in Figure 6 at ambient temperature after the chemical oxidation without trifluoroacetic anhydride. The simulation assuming $\Delta B_{1/2} = 0.285$ mT, $a_N = 0.3$ mT, and $a_H = 0.26$ mT reproduced the observed one as shown in Figure 5a. The hyperfine coupling parameters for three equivalent nitrogen and hydrogen atoms were taken into

(26) Luckhurst, G. R.; Pedulli, G. F.; Tiecco, M. *J. Chem. Soc. B* **1971**, 329−334.
(27) Kothe, G.; Denkel, K.-H.; Sümmermann, W. *Angew. Chem., Int. Ed. Engl.* **1970**, *9*, 906−907.
(28) Veciana, J.; Rovira, C.; Crespo, M. I.; Armet, O.; Domingo, V. M.; Palacio, F. *J. Am. Chem. Soc.* **1991**, 113, 2552−2561.

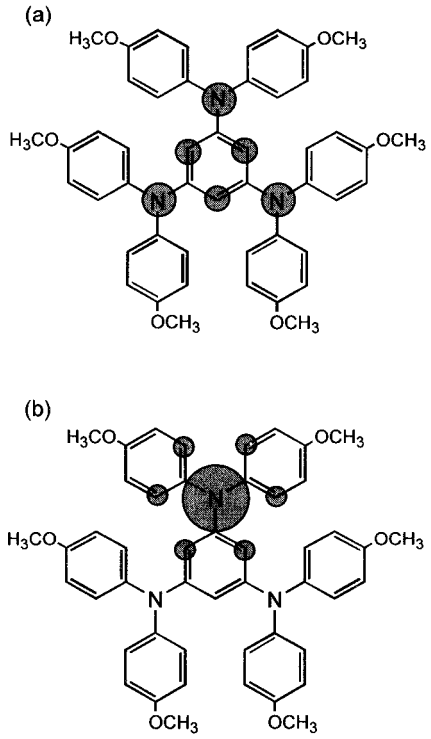

Figure 7. Probable spin structures expected for the polycationic and monocationic states of **2**. The area of the circle denotes only relative spin densities on the carbon and nitrogen atomic sites.

account. The solution ESR spectrum that was observed with trifluoroacetic anhydride is expected to be due to the tricationic state of **2**. On the other hand, the spectrum in Figure 6a was simulated assuming the following parameters: $\Delta B_{1/2} = 0.64$ mT, $a_N = 0.7$ mT (for one of three nitrogen atoms), and $a_N = 0.01$ mT (for the other nitrogen atoms). The line width used for the spectral simulation in Figure 6b was larger than that in Figure 5. In the spectral simulation of Figure 6a, we did not take the hyperfine couplings arising from the hydrogen atoms into account. The line width suggested that the hyperfine couplings from the hydrogen atoms cause the spectral line broadening. The species giving rise to the ESR spectrum shown in Figure 6 was extremely stable, and the spectrum survived a week after the sample was kept at ambient temperature. Since the monocation of *para*-substituted triphenylamine was well known as a persistent radical,[29] the monocationic state of **2** was supposed to be stable at ambient temperature. This also gives a rationale for our assignment that the ESR spectrum is due to the monocationic state of **2**. The persistent monocationic state is consistent with the results of cyclic voltammetry experiments that were performed in order to examine the stability of the tricationic state of **2** and its analogues.[30]

The probable spin structures of the tricationic and monocationic states based on the spectral simulations are given in parts a and b, respectively, of Figure 7. The area of the circle denotes only relative spin densities on the carbon and nitrogen atomic sites. The former was estimated from the McConnell equation $\rho_\pi = a/Q$ ($Q = -66.9$ MHz[31]). The unpaired electron spin is delocalized over the diarylamino moieties in the polycationic state of **2**, giving the same isotropic hyperfine coupling parameters from three nitrogen atoms. The hyperfine coupling

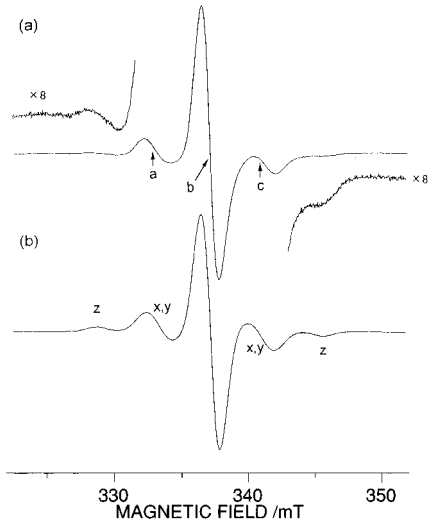

Figure 8. (a) Powder-pattern ESR spectrum of the tricationic state of **2** observed at 7 K. The microwave frequency was 9.44751 GHz. (b) Simulated ESR spectrum with $S = 3/2$, $g = 2.0023$, $|D| = 0.004$ cm^{-1}, $|E| = 0.0002$ cm^{-1}, $\Delta B_{1/2} = 1.0$ mT, $a_N = 0.32$ mT (for three nitrogen atoms), and $a_H = 0.28$ mT (for three hydrogen atoms of the central phenyl ring).

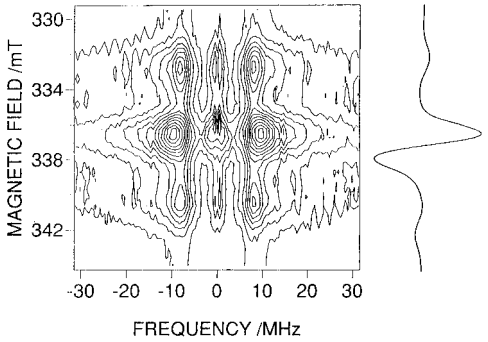

Figure 9. Contour plot of the field-swept 2D ESTN spectra of $\mathbf{2}^{3(\bullet+)}$ and the conventional field-swept ESR spectrum (on the right) observed at 6 K. ω_1 corresponds to about 5 MHz.

parameters from three hydrogen atoms were assigned to those of the central phenyl ring, resulting from electron−nuclear interactions between the hydrogen atom and electron spin on neighboring carbon sites. The carbon sites on the central phenyl ring have large π-spin densities that are additively brought from each diarylamino moiety by the spin polarization mechanism. On the other hand, in the monocationic state of **2** the electron spin is localized to one of the diarylamino moieties. The spin structure of the monocationic state is essentially similar to that of triphenylamine as a persistent radical monocation.

Tricationic State of 2. Figure 8a shows the powder-pattern ESR spectrum of $\mathbf{2}^{3(\bullet+)}$ observed at 7 K in the dichloromethane glass. There appeared five broad lines in the allowed ESR transition region. They were assigned to canonical peaks arising from the quartet spin state with $|D| = 0.004$ cm^{-1}, $|E| = 0.0002$ cm^{-1}, and $g = 2.0023$ (isotropic). The simulation spectrum is shown in Figure 8b. From the simulation, $a_N = 0.32$ mT and $a_H = 0.28$ mT were derived for three nitrogen atoms and for three hydrogen atoms of the central phenyl ring, respectively.

In order to identify the molecular spin multiplicity of the cationic state, we carried out the ESTN measurements. Figure 9 shows a contour plot of 2D-ESTN spectra of $\mathbf{2}^{3(\bullet+)}$ observed at 6 K. The intense nutation frequency peak observed at 336.8 mT and two peaks at 333 and 340.4 mT are at 10.08 and 8.12 MHz, respectively. A ratio of the observed nutation frequencies, 10.08/8.12, agrees with that of $2/\sqrt{3}$ expected for a quartet spin

(29) Seo, E. T.; Nelson, R. F.; Fritsch, J. M.; Marcoux, L. S.; Leedy, D. W.; Adams, R. N. *J. Am. Chem. Soc.* **1966**, *88*, 3498−3503.

(30) Yano, M.; Furuichi, M.; Sato, K.; Shiomi, D.; Ichimura, A.; Abe, K.; Takui, T. and Itoh, K. *Synth. Met.* **1997**, *85*, 1665−1666.

(31) Hirota, N; Hutchison Jr., C. A.; Palmer, P. *J. Chem. Phys.* **1964**, *40*, 3717−3725.

state from eq 4. We can, therefore, assign the intense peak and two weak ones to $|3/2, 1/2\rangle \leftrightarrow |3/2, -1/2\rangle$ and $|3/2, \pm 3/2\rangle \leftrightarrow |3/2, \pm 1/2\rangle$ allowed transitions of a pure quartet state,[32] respectively. In the 2D-ESTN spectra no peaks were observed at 5 MHz (ω_1) which corresponded to the $S = 1/2$ nutation frequency. This illustrates straightforwardly that the quartet state is a ground state. If the quartet state is an excited one, the frequency component ω_1 arising from a doublet ground state has to be observed.[33] If the energy gap between the doublet and quartet states is comparable to 0.3 cm^{-1}, effects of spin quantum mixing appear appreciable in fine-structure spectra. The mixed-doublet peak from organic species is expected to appear at the $g \approx 2$ region with a reduced intensity.[32] The 2D-ESTN experiments in the wide range of temperature indicate that an excited doublet state can be located higher than 100 cm^{-1} above the quartet ground state.

For some quartet cases only, apparently missing Z peaks due to line broadening in glasses resemble triplet fine-structure spectra: This was not the case for the spectra of $\mathbf{2}^{\mathbf{3(\bullet+)}}$. Referred to fine-structure forbidden transitions, $\Delta M_S = \pm 2$ transitions from a quartet species often interfere with those from triplet species, making identification of the transitions from quartet species difficult. The forbidden transitions are masked with a strong peak due to undesired triplet species. Particularly, the $\Delta M_S = \pm 2$ peak due to small D values is misleading in S-discrimination between triplet and quartet states. On the other hand, the absorption peak arising from $\Delta M_S = \pm 3$ forbidden transitions can show fingerprint evidence of quartet states. Their transition probability, nevertheless, is small in 1 or 2 orders of magnitude. This trend is enhanced with decreasing fine-structure parameters.

The S/M_S-identification and mapping of transition assignments based on the 2D-ESTN spectroscopy are free from the above weakness of cw ESR spectroscopy applied to high-spin chemistry.

The determined $|D|$ value of 0.0040 cm^{-1} is also close to that of a neutral quartet molecule with hyperbranched diaryl-based spin structures,[34] being consistent with the results from $\mathbf{1}^{\mathbf{2(\bullet+)}}$. The ESTN measurements are underway on sizable poly(triarylamine)-based analogues that have undergone incomplete oxidation in solution,[35] leading to complex cw ESR fine-structure spectra in organic glasses.

Conclusions

The field-swept 2D ESTN spectroscopy as a novel ESR technique unequivocally showed that the di- and tricationic states of **1** and **2** are a ground-state triplet and quartet, respectively, indicating that these ground-state high spins originate from the topological pseudodegeneracy of the π-HOMOs which governs spin alignment in polycationic heteroatomic systems. The electronic spin structures of the cationic states of **2** were determined on the basis of the hyperfine coupling parameters. The model system $\mathbf{1}^{\mathbf{2(\bullet+)}}$ is the first example for one-dimensional high-spin polycations. It is illustrated that the 2D ESTN spectroscopy is a powerful and facile method for spin identification and discrimination between different spin multiplicities in nonoriented systems.

Acknowledgment. This work has been partially supported by Grants-in-Aid for Scientific Research on Priority Area "Molecular Magnetism" (Area Nos. 228/04242103 and 04242105) and Grants-in-Aid for Encouragement of Young Scientists (Grant Nos. 07740468, 08740462 (K.S.), and 07740553 (D.S.)) from the Ministry of Education, Science and Culture, Japan, and also by the Ministry of International Trade and Industries (NEDO project "Organic Magnets").

JA963372+

(32) Fine-structure ESR spectra arising from spin quantum mixing of a triplet and a doublet state differ from pure spin-quartet spectra, particularly transition-intensity borrowing due to the mixing taking place. Fine-structure ESR spectroscopy from spin quantum mixing has been documented.[25]

(33) The central nutation frequencies appearing at ~0 MHz in Figures 3 and 9 contain contributions from double/triple quantum transitions feasibly occurring in high-spin systems. The nutation frequencies intrinsic to multiple quantum transitions are predicted to appear near 0 MHz.[23]

(34) Veciana, J.; Rovira, C.; Ventosa, N.; Crespo, M. I.; Palacio, F. *J. Am. Chem. Soc.* **1993**, *115*, 57−64.

(35) Blackstock, S. C. Personal communication.